

## Selective quasienergies from short time cross-correlation probability amplitudes by the filter-diagonalization method

Markus Glück,<sup>1</sup> H. Jürgen Korsch,<sup>1</sup> and Nimrod Moiseyev<sup>2</sup>

<sup>1</sup>*Fachbereich Physik, Universität Kaiserslautern, D-67653 Kaiserslautern, Germany*

<sup>2</sup>*Department of Chemistry and Minerva Center for Non Linear Physics of Complex Systems, Technion, Israel Institute of Technology, Haifa 32000, Israel*

(Received 28 August 1997; revised manuscript received 20 March 1998)

The filter-diagonalization method is applied to time periodic Hamiltonians, and used to find selectively the regular and chaotic quasienergies of a driven two-dimensional rotor. The use of  $N$  cross-correlation probability amplitudes enables a selective calculation of the quasienergies from short time propagation to the time  $T^{(N)}$ . Compared to the propagation time  $T^{(1)}$  which is required for resolving the quasienergy spectrum with the same accuracy from autocorrelation calculations, the cross-correlation time  $T^{(N)}$  is shorter by the factor  $N$ , that is  $T^{(1)} = NT^{(N)}$ . [S1063-651X(98)01307-5]

PACS number(s): 05.45.+b, 03.65.-w

### I. INTRODUCTION

Filter diagonalization was recently introduced by Neuhauser [1] and Neuhauser and co-workers [2–4] as a general method to extract frequencies (poles) from a given signal. The approach has been extensively used, in quantum dynamics and general contexts, by several groups [5–7]. In the calculation of photoabsorption probabilities, filter diagonalization together with the  $(t, t')$  method, has been used as an effective tool to extract quasienergies from the autocorrelation function without full-matrix diagonalization [8].

Recently it was proposed to extract the energy spectrum of the studied system from the cross-correlation functions rather than from the autocorrelation amplitudes [1,9]. This approach enables us [9] to extract the resonance positions and widths (associated with the complex eigenvalues of the complex scaled Hamiltonian) from very short time propagations which are too short to obtain the spectrum from autocorrelation calculations.

Mandelshtam and Taylor's simple box filter [5] was found to be very efficient, and we will also use it in the present application of the filter diagonalization method with cross-correlation functions to time periodic Hamiltonians. In particular, we will show the following.

(a) The filter-diagonalization method is applicable to time periodic Hamiltonians,  $H(t) = H(t+T)$ , provided the autocorrelation and cross-correlation amplitudes are calculated or measured at  $t = T, 2T, 3T, \dots$  and *not* at any other time interval.

(b) The quasienergy (QE) spectrum can be extracted either from the autocorrelation or cross-correlation amplitudes.

(c) The QE's which are predominantly populated by the initial state(s) are most accurately obtained. When the initial states are localized in the chaotic regime of the classical phase space, all chaotic QE states are obtained, whereas regular QE states are obtained when the initial states are localized in the regular part of the stroboscopic Poincaré surface of section.

(d) Accurate QE spectra can be obtained from  $N$  cross-correlation functions propagated from  $t=0$  to  $t=mT$ ,

whereas  $N$  times more propagation steps (i.e. up to  $t = mNT$ ) are required in order to obtain an accurate spectrum from  $N$  autocorrelation amplitudes.

This allows us to replace one long time calculation by a few short time calculations, which is a useful tool in systems for which the numerical effort of long time calculations increases with time, or for which only the short time regime yields significant information, e.g., in the calculation of fast decaying resonances [9].

### II. FILTER DIAGONALIZATION FOR TIME PERIODIC HAMILTONIANS

The filter-diagonalization method enables one to calculate selectively the energy spectrum of time independent systems from the autocorrelation amplitudes,

$$C_n(t) = \langle \phi_n | \hat{U}(t) | \phi_n \rangle, \quad (1)$$

or from the cross-correlation amplitudes,

$$C_{n,m}(t) = \langle \phi_n | \hat{U}(t) | \phi_m \rangle, \quad (2)$$

where  $\hat{U}(t)$  is the time evolution operator,  $n, m \in \{1, 2, \dots, N\}$  [9], and  $t < \mathcal{T}$ . The key point is that the time  $\mathcal{T}$  is too short to obtain the spectrum by fast Fourier transform or by other known methods [1–5]. The energy eigenvalues of the system,  $E$ , are obtained by solving a generalized eigenvalue problem

$$\mathbf{U}\vec{\Psi} = \lambda \mathbf{S}\vec{\Psi}, \quad (3)$$

where  $\mathbf{U} = \mathbf{U}(\Delta t)$  is the time propagator for a time step  $\Delta t$ , and  $\mathbf{S}$  is the overlap matrix of the filter basis functions. Both matrices consist of  $N \times N$  submatrices with the dimension  $N_f \times N_f$ , where  $N$  is the number of initial states for the cross-correlation amplitudes and  $N_f$  the number of filter basis func-

tions (for further details, see Ref. [9]). We should emphasize that the *only* input data needed to calculate  $\mathbf{U}$  and  $\mathbf{S}$  are  $C_n(t)$  or  $C_{n,m}(t)$  at the discrete times  $t=k \Delta t$ ,  $k=0,1,2,\dots,N_t$ , where  $N_t \Delta t = \mathcal{T}$ . There is no need to know even for which Hamiltonian system  $C_n(t)$  [or  $C_{n,m}(t)$ ] were calculated or measured. The eigenvalues and the energy spectrum are related by  $E=i\hbar(\Delta t)^{-1} \ln(\lambda)$  [9] (note that the quasienergies are defined up to multiples of  $\hbar\omega$ ). The derivation of Eq. (3) for time independent systems is based on two facts.

(I) The energy eigenstates  $|\Phi_E\rangle$  of the Hamiltonian  $\hat{H}$  are also eigenstates of the time evolution operator  $\hat{U}(t) = \exp(-i\hat{H}t/\hbar)$ ,

$$\hat{U}(t)|\Phi_E\rangle = \exp(-iEt/\hbar)|\Phi_E\rangle. \quad (4)$$

(II) The filter basis functions, which are taken as a basis set to diagonalize the time evolution operator  $\hat{U}$ , are defined as

$$|\Phi_E\rangle = \frac{1}{\mathcal{T}} \int_0^{\mathcal{T}} dt e^{iEt/\hbar} \hat{U}(t)|\phi(0)\rangle. \quad (5)$$

In the limit  $\mathcal{T} \rightarrow \infty$  they are eigenstates if  $E$  is an eigenvalue.

For time dependent systems the first condition is, of course, not fulfilled, since the time evolution operator is *not*  $\exp[-i\hat{H}(t)t/\hbar]$ . We can overcome this difficulty by expressing the time evolution operator by the  $(t, t')$  method [10]. This implies that the Hamiltonian  $\hat{H}$  in the first conditions and in the expressions used to derive Eq. (3) (see Ref. [9]) should be replaced by the Floquet or quasienergy operator  $\hat{\mathcal{H}} = \hat{p}_{t'} + \hat{H}(t')$  which is time (i.e.,  $t$ ) independent. Here  $t'$  acts as an additional coordinate and not as a parameter. The momentum operator  $\hat{p}_{t'}$  is defined as usual. Using  $(t, t')$ , we can obtain an analytical form of the time evolution operator,

$$\hat{U}(t) = \int dt' \delta(t-t') \exp[-i\hat{\mathcal{H}}(t') t/\hbar]. \quad (6)$$

This fact enables the derivation of time independent scattering theory for time dependent Hamiltonians [10,11]. Let us now check if the above mentioned conditions are fulfilled for time periodic systems.

(I) For time periodic Hamiltonians, the quasienergy solutions  $|\Psi_E\rangle$  (which are defined as eigenstates of the Floquet operator) are given by

$$\hat{\mathcal{H}}(t)|\Psi_E(t)\rangle = E|\Psi_E(t)\rangle \quad (7)$$

with the time periodic functions

$$|\Psi_E(t)\rangle = |\Psi_E(t+T)\rangle. \quad (8)$$

On the other hand, using Eq. (6),

$$\hat{U}(t)|\Psi_E(0)\rangle = e^{-iEt/\hbar}|\Psi_E(t)\rangle, \quad (9)$$

so that condition (I) [see Eq. (4)] is fulfilled if  $|\Psi_E(0)\rangle = |\Psi_E(t)\rangle$ , which is only the case for  $t=nT$  [see Eq. (8)].

(II) As condition (I) is fulfilled only at the discrete times  $t=nT$ ,  $n=0,1,2,\dots$ , the integration in the definition of the

filter basis functions [Eq. (5)] has to be replaced by a summation. So, for time periodic Hamiltonians, the filter basis functions are given by

$$|\Psi_E\rangle = \frac{1}{N_t+1} \sum_{n=0}^{N_t} e^{inET/\hbar} \hat{U}(nT)|\phi(0)\rangle. \quad (10)$$

Using this definition, we see that in the limit  $N_t \rightarrow \infty$  the filter basis function  $\Psi_E$  is an eigenfunction of the Floquet operator if  $E$  is a quasienergy, and condition (II) is fulfilled.

This shows that in the case of time periodic Hamiltonians we have to take  $\Delta t = T$  and modify the definition of the filter basis functions. Only then can the QE spectrum be obtained by the filter-diagonalization method. This conclusion has been confirmed by our numerical calculations.

### III. SELECTIVE QUASIENERGIES FROM SHORT TIME CROSS CORRELATIONS

Let us take as an illustrative numerical example a two-dimensional (2D) driven rotor Hamiltonian

$$\hat{H}(t) = \frac{\hat{p}_\phi^2}{2} + \cos(\phi)\cos(\omega t) \quad (11)$$

modeling, e.g., a dipole in an oscillating field (the rotational momentum  $\hat{p}_\phi$  is  $\hbar m$ , where  $m \in \{0, \pm 1, \pm 2, \dots\}$  is the rotational quantum number). This system, also known as the double resonance model, is one of the models investigated extensively in context with quantum chaos (see, e.g., Refs. [12–17]).

The classical dynamics of system (11) is chaotic, i.e., it shows a mixture of regular and chaotic dynamics. Stroboscopic Poincaré sections of the classical phase space at  $t=nT$ , ( $n=0,1,2,\dots$ ) are shown in Fig. 1 for the frequencies  $\omega=0.6$  and  $\omega=1.2$ . For  $\omega=0.6$  we have a clear division of phase space into a single inner chaotic and two outer regular regions. For  $\omega=1.2$  two inner (classically disconnected) regular islands appear, centered at the two stable resonant corotating and counter-rotating periodic modes of the rotor.

In quantum studies, it has been found that in the semiclassical regime the quasienergy states can be divided into two classes of eigenstates [15,17]. One class of solutions comprises extended quasienergy states which almost uniformly populate the free rotor states below a specific value of  $|m|$  in 2D problems and below the rotational quantum number  $j$  in the 3D case (see Figs. 7, 17, and 18 in Ref. [15] and Fig 10(a) in Ref. [16]). The strong random population of all contributing free rotor basis functions is reflected in the Husimi distribution, which shows almost an equal probability in the classically chaotic region (see Fig. 10(b) in Ref. [16]). The states which belong to this class of solutions are referred to as *chaotic* quasienergy states.

The second class of solutions, which are referred to as *regular* states, is localized both in the free rotor basis set and in the stroboscopic Poincaré surface of sections. See Fig. 6 in Ref. [16] for states the Husimi distribution of which is localized in the inner regular islands of the chaotic ‘‘sea,’’ and Fig. 9 in Ref. [16] for states which are localized along outer regular orbits.

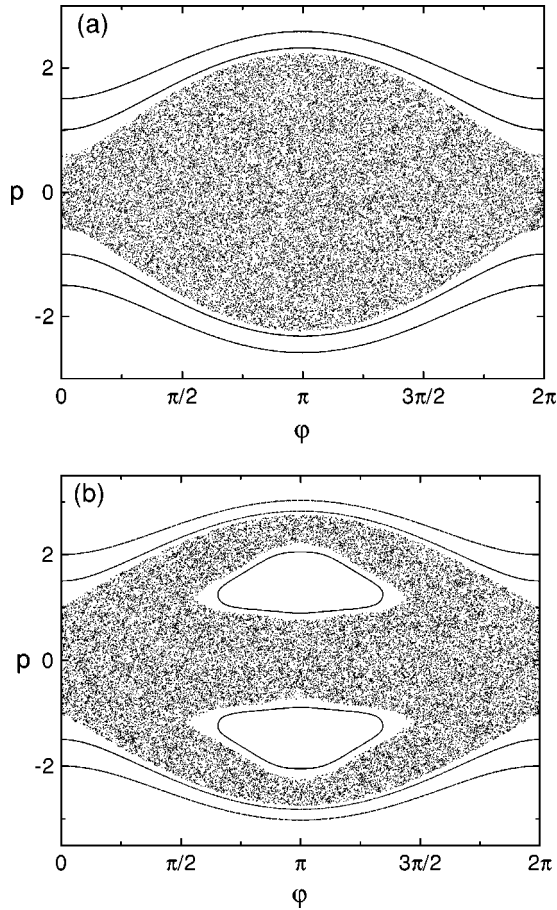


FIG. 1. Stroboscopic Poincaré section of classical phase space at  $t = nT$ , ( $n = 0, 1, 2, \dots$ ). All points in the chaotic region result from one single classical trajectory: (a) driven rotor with the frequency  $\omega = 0.6$ , (b) driven rotor with the frequency  $\omega = 1.2$ .

The quasienergies for  $\hbar = 0.1$  and  $\omega = 0.6$ , and also for  $\omega = 1.2$ , were calculated using 81 free rotor states as a basis set. The numerically exact quasienergies (chaotic and regular following the definitions given above) were obtained from the diagonalization of the Floquet time evolution operator  $\hat{U}(T)$ . Forty of these states could be classified as chaotic, in agreement with the estimate from the area of the chaotic region in phase space. The quasienergies of chaotic states for  $\omega = 0.6$  in the representative interval  $0.01 < E < 0.02$  are given in the *second* column of Table I.

To demonstrate the selectivity of the filter-diagonalization method, we first compute *only* the chaotic quasienergy states. As the chaotic quasienergy states almost uniformly populate the free rotor states, conversely the free rotor states almost uniformly populate the chaotic QE states. Thus we expect to populate all chaotic states using the  $n = 0, 1, 2, 3$ , and 4 free rotor states as initial states. We calculated the spectrum from the autocorrelation functions  $C_n(t)$  with  $n = 0, 1, 2, 3$ , and 4, and also from the cross-correlation amplitudes  $C_{n,m}(t)$ , where  $n, m = 0, 1, 2, 3$ , and 4.

For the first calculation, the Neuhauser method [2] with a Mandelshtam-Taylor filter was used. The recent generalization of the filter method by Narevicius, *et al.* [9] was used to extract the quasienergy spectrum from the cross-correlation functions. The results for  $\omega = 0.6$  are presented in Table I.

The *first* lines in boxes of the *third* column of the table are

the chaotic quasienergies obtained from *long* time propagated autocorrelation functions  $C_n(t)$ , where  $t = 0, T, 2T, \dots, 100T$ . The reason for sampling the autocorrelation functions every time period has been explained above. The results obtained from *short* time propagated autocorrelation functions with  $t = 0, T, 2T, \dots, 20T$  are presented in the *third* (last) lines of the boxes in the *third* column of Table I.

The deviation of the quasienergies obtained by the filter-diagonalization method from the exact values are shown in the *last* column in Table I. The results obtained from *long* time (100T) propagations are in a remarkable agreement with the exact values. Note that the Fourier transform of the same functions provide results, which are less accurate by several orders of magnitudes.

The results obtained from the *short* time (20T) propagation are poor. In some cases it was impossible to allocate a spectral line from the analysis of the autocorrelation functions to the exact QE value. In the best case, *short* time results were less accurate by more than four orders of magnitude from the the long time result.

The imaginary part of the QE should be equal to zero as the QE states are bounded states, so we use the imaginary part of the calculated QE (the *fourth* column in Table I) as an independent error estimate of the filter diagonalization. Another error estimate can be obtained from the variations of the spectral lines (the *fifth* column in Table I) as the time evolution operator was diagonalized by the filter method at  $t = T, 2T$ , and  $3T$  (for a more detailed explanation, see Refs. [5] and [9]). Comparing the last three columns, the independent errors are about equal to the actual error of the results.

It is interesting to compare the errors of the long time autocorrelation results with the the population of the quasienergy states by the initial states (the *first* column in Table I). An error of  $3.38 \times 10^{-9}$  was obtained for the state populated at the probability of 0.000 474, while an error of  $5.39 \times 10^{-11}$  was obtained for a state populated at a higher probability of 0.0819. Another interesting result that will be discussed later in more detail is that the *largest* errors are obtained for *almost degenerate states*.

The rationale behind the success of the filter-diagonalization method to extract the QE spectrum from the long time propagated autocorrelation functions, and its failure to do so for the short time propagation, is as follows. Each one of the QE states fills up a specific region in the classical phase space. The minimal time which is required to extract the QE value from  $C_n(t)$  is the time it takes for the  $n$ th initial state to cover entirely this specific region in the classical phase space (this can be seen by carrying out time dependent Husimi distribution calculations). Our results clearly show that 20T is not enough to do so, but 100T is more than enough.

Following this rationale, we expect that in the case of  $N \times N$  cross-correlation calculations the  $N$  initial states *together* will cover the entire bounded chaotic classical phase space within  $100/N$  periods. That is, for  $N = 5$  it is enough to calculate (or to measure)  $C_{n,m}$  with  $n, m = 0, 1, 2, 3$ , and 4 up to  $t = 20T$ . The results of this calculation are presented in the *second* lines of the boxes in the *third* column in Table I. The results are in excellent agreement with the exact QE values,

TABLE I. Numerically exact quasienergies and results obtained by the filter-diagonalization method using long time autocorrelation (*first rows*, 100 periods), short time cross-correlation (*second rows*, 20 periods) and short time autocorrelation amplitudes (*third rows*, 20 periods) as input data.  $\Delta(E)$  denotes the deviations from the numerically exact values.  $\text{Im}(E)$  is the imaginary part, and Err. is the error estimate obtained in the filter diagonalization procedure (see the text). Pop. is the summed population probability of the QE state by the initial states used in the propagation.

Pop	$E(\text{exact})$	$E(\text{filter})$	$\text{Im}(E)$	Err.	$\Delta E$
$1.51 \times 10^{-1}$	0.010 616 379 394 2	0.010 616 379 231 2	$-3.07 \times 10^{-10}$	$6.84 \times 10^{-10}$	$1.63 \times 10^{-10}$
		0.010 616 412 758 8	$-2.24 \times 10^{-8}$	$8.07 \times 10^{-8}$	$3.34 \times 10^{-8}$
		none	—	—	—
$1.87 \times 10^{-1}$	0.011 177 375 893 1	0.011 177 375 912 7	$2.59 \times 10^{-11}$	$1.69 \times 10^{-10}$	$1.96 \times 10^{-11}$
		0.011 177 312 582 7	$1.67 \times 10^{-7}$	$3.56 \times 10^{-7}$	$6.33 \times 10^{-8}$
		0.011 416 196 078 1	$-7.72 \times 10^{-4}$	$2.76 \times 10^{-4}$	$2.39 \times 10^{-4}$
$9.49 \times 10^{-2}$	0.013 528 743 941 0	0.013 528 750 836 8	$-3.12 \times 10^{-9}$	$1.18 \times 10^{-9}$	$6.90 \times 10^{-9}$
		0.013 528 904 318 8	$2.59 \times 10^{-9}$	$3.11 \times 10^{-7}$	$1.60 \times 10^{-7}$
		none	—	—	—
$4.74 \times 10^{-4}$	0.013 623 787 067 0	0.013 623 790 442 9	$-4.83 \times 10^{-9}$	$1.11 \times 10^{-8}$	$3.38 \times 10^{-9}$
		0.013 623 796 403 4	$-2.60 \times 10^{-7}$	$5.02 \times 10^{-7}$	$9.34 \times 10^{-9}$
		none	—	—	—
$4.20 \times 10^{-2}$	0.013 660 580 464 0	0.013 660 557 568 1	$-1.35 \times 10^{-8}$	$5.42 \times 10^{-8}$	$2.29 \times 10^{-8}$
		0.013 660 864 532 0	$1.40 \times 10^{-7}$	$5.74 \times 10^{-7}$	$2.84 \times 10^{-7}$
		0.013 839 372 992 5	$4.67 \times 10^{-3}$	$5.99 \times 10^{-3}$	$1.79 \times 10^{-4}$
$2.04 \times 10^{-1}$	0.014 161 221 382 8	0.014 161 221 683 0	$3.75 \times 10^{-10}$	$1.08 \times 10^{-9}$	$3.00 \times 10^{-10}$
		0.014 161 238 074 3	$6.92 \times 10^{-9}$	$3.54 \times 10^{-8}$	$1.67 \times 10^{-8}$
		0.014 539 644 122 1	$-5.65 \times 10^{-5}$	$1.21 \times 10^{-4}$	$3.78 \times 10^{-4}$
$8.19 \times 10^{-2}$	0.016 968 394 762 0	0.016 968 394 815 9	$3.16 \times 10^{-11}$	$3.56 \times 10^{-10}$	$5.39 \times 10^{-11}$
		0.016 968 390 345 6	$-7.97 \times 10^{-9}$	$1.65 \times 10^{-8}$	$4.42 \times 10^{-9}$
		0.017 683 921 754 4	$6.29 \times 10^{-4}$	$3.05 \times 10^{-4}$	$7.16 \times 10^{-4}$
$2.43 \times 10^{-1}$	0.018 915 768 674 6	0.018 915 769 457 8	$1.56 \times 10^{-11}$	$3.36 \times 10^{-10}$	$7.83 \times 10^{-10}$
		0.018 915 748 596 2	$5.19 \times 10^{-8}$	$1.13 \times 10^{-7}$	$2.01 \times 10^{-8}$
		0.018 745 383 620 3	$8.93 \times 10^{-5}$	$1.17 \times 10^{-4}$	$1.70 \times 10^{-4}$
$1.39 \times 10^{-1}$	0.019 538 017 165 5	0.019 538 018 107 4	$-1.07 \times 10^{-10}$	$8.94 \times 10^{-10}$	$9.42 \times 10^{-10}$
		0.019 537 888 467 3	$9.43 \times 10^{-8}$	$3.19 \times 10^{-7}$	$1.29 \times 10^{-7}$
		0.019 550 056 755 5	$-4.91 \times 10^{-4}$	$7.23 \times 10^{-4}$	$1.20 \times 10^{-5}$

and far better than the results obtained from the short time (also  $20T$ ) propagations of the five separated autocorrelation functions.

This is observed for all chaotic QE solutions in Fig. 2, where the errors in the QE are shown vs the computed QE values. The results obtained from the short time propagated cross-correlation data are more accurate over several orders of magnitude (on the average by 4) than the results computed from the short time propagated autocorrelation amplitudes.

In order to show that indeed *all* chaotic QE's were obtained by the filter-diagonalization method using five short time ( $20T$ ) propagated cross-correlation functions, in the upper part of Fig. 3 we plot the exact QE values and their summed population by the five initial states, whereas in the lower part of Fig. 3 the QE spectrum obtained by the filter diagonalization and the corresponding values of the inverse of the error are plotted. In Fig. 4, for comparison, we show the same plot for the results obtained by the filter-diagonalization method from the short time propagated autocorrelation functions (the long time autocorrelation functions provide good results as in Fig. 3). Unlike the results presented in Fig. 4, the QE spectrum obtained from the five short time propagated cross-correlation functions (Fig. 3) is very accurate. In the scale of the plot of Fig. 3, all of the QE's are not only indistinguishable from the exact values, but the small errors are also proportional to the inverse of the

populations of the QE by the initial states. That is, as the populations become larger, the error is smaller.

Following the rationale behind the success of filtering out the QE spectrum from short time propagations of cross-

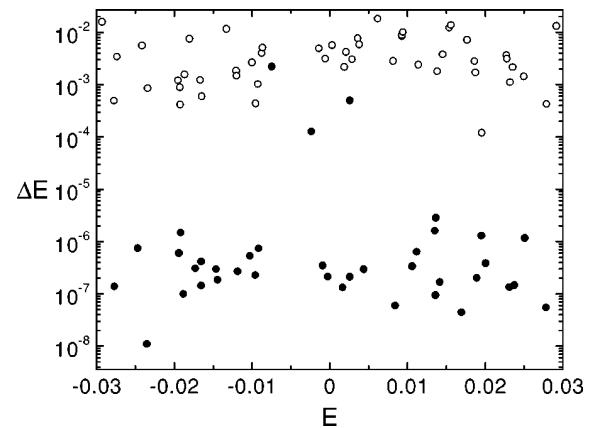


FIG. 2. The deviation of the quasienergies obtained by the filter-diagonalization method from the exact numerical values. The open circles (large error) were obtained by filtering out the spectrum from the short time (20 periods) propagation of five different autocorrelation amplitudes. The full circles (small error) were obtained from five cross-correlation function amplitudes.

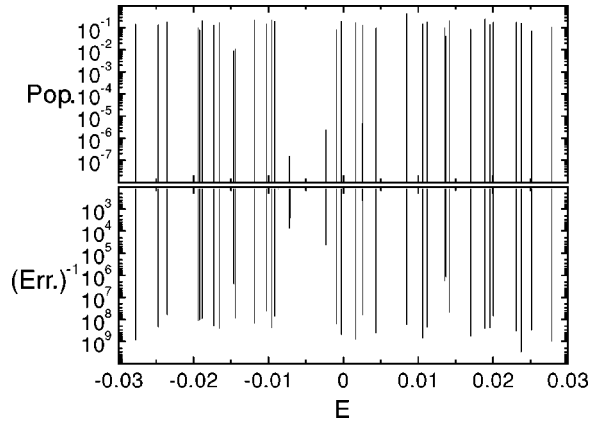


FIG. 3. The upper plot shows the numerically exact quasienergy spectrum and the summed population probabilities of the initial states used in the time propagation calculations. The lower plot shows the QE spectrum obtained by the filter-diagonalization calculations using the five short time propagated cross-correlation amplitudes vs the inverse of the calculated error estimate. Both spectra show excellent agreement.

correlation functions one, may expect that this will be the most efficient procedure for calculating a regular QE since the QE state is localized in a relatively small region of the stroboscopic Poincaré surface of section. This is indeed the situation. However, there are cases, as shown in Fig. 1(b), that, due to the symmetrical pair of regular islands, the regular part of the spectrum (associated with the regular QE states) is almost degenerate. The results presented in Table II clearly show that five short time propagation calculations with cross-correlation functions cannot resolve the splitting. To obtain better results, one has to increase the time interval, e.g., for  $t=100T$  the agreement is much better (see the last column of Table II). It is interesting to compare the propa-

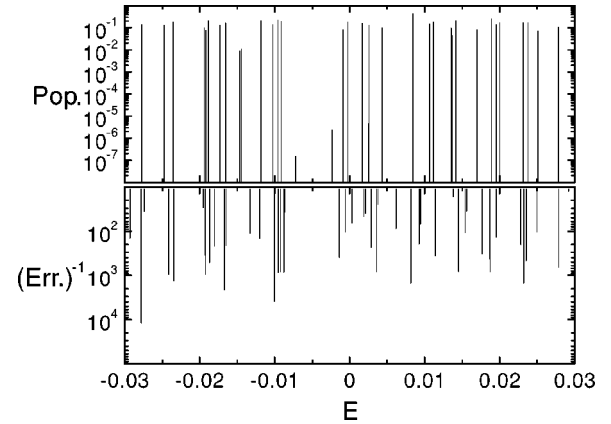


FIG. 4. As in Fig. 3, but five separated short time propagated autocorrelation amplitudes were used as an input data in the filter-diagonalization method. The agreement of the spectra is bad.

gation time with the ‘‘tunneling time’’  $\tau = \pi\hbar/\Delta(\pm)$  (the *second* column in Table II), where  $\Delta(\pm)$  stands for the energy splitting. We find that filter diagonalization with cross-correlation amplitudes can resolve splittings even if the propagation time is remarkably shorter than the tunneling time.

#### IV. CONCLUDING REMARKS

Using the filter-diagonalization method when the input data are time dependent cross-correlation functions sampled at  $t=T, 2T, \dots$  highly accurate quasienergy spectra of time periodic systems can be obtained. The error is smaller for QE’s that are more highly populated by the initial states, and larger for almost degenerate states. As a rule of thumb we may conclude that, as more initial states are used to calculate the cross-correlation amplitudes, one can filter out an accurate QE spectrum from shorter time propagation calculations.

TABLE II. Five pairs of almost degenerate regular quasienergies and results obtained by the filter-diagonalization method when the long time (100 periods) and short time (20 periods) propagated cross-correlation amplitudes are used as input data.  $\Delta(\pm)$  stands for the energy splitting between any two almost degenerate QE states,  $\tau$  denotes the tunneling time  $\tau = \pi\hbar/\Delta(\pm)$ .

$\Delta(\pm)$	$\tau/T$	$E(\text{exact})$	$E(20T)$	$E(100T)$
$3.55 \times 10^{-9}$	$1.69 \times 10^7$	0.027 232 623 10	0.027 232 623 10	
		0.027 232 626 65		0.027 232 626 08
$2.49 \times 10^{-7}$	$2.41 \times 10^5$	-0.022 735 476 56	-0.022 735 595 70	-0.022 735 601 66
		-0.022 735 725 71		-0.022 744 783 76
$1.54 \times 10^{-5}$	$3.90 \times 10^3$	0.045 859 222 47	0.045 866 882 80	0.045 859 655 74
		0.045 874 534 32		0.045 875 015 85
$7.73 \times 10^{-4}$	$7.75 \times 10^1$	-0.006 575 290 61	-0.006 842 989 47	-0.006 575 283 41
		-0.007 351 527 21		-0.007 351 533 32
$1.03 \times 10^{-3}$	$5.83 \times 10^1$	0.057 706 791 31	0.057 646 876 57	0.057 706 791 16
		0.058 739 703 81	0.058 703 565 60	0.058 739 703 89

## ACKNOWLEDGMENTS

This work was done while one of the authors (N.M.) was staying at the University of Kaiserslautern. The U.S.–Israel Binational Foundation and the Foundation of Promotion of

Research at the Technion are acknowledged for partial support. This research was supported by the Deutsche Forschungsgemeinschaft (SPP “Zeitabhängige Phänomene und Methoden in Quantensystemen der Physik und Chemie”).

- 
- [1] D. Neuhauser, J. Chem. Phys. **93**, 2611 (1990).  
[2] M. R. Wall and D. Neuhauser, J. Chem. Phys. **102**, 8011 (1995).  
[3] G.-J. Kroes, M. R. Wall, J. W. Pang, and D. Neuhauser, J. Chem. Phys. **106**, 1800 (1997).  
[4] J. W. Pang and D. Neuhauser, Chem. Phys. Lett. **252**, 173 (1996).  
[5] V. A. Mandelshtam and H. S. Taylor, J. Chem. Phys. **106**, 5085 (1997); Phys. Rev. Lett. **78**, 3274 (1997); J. Chem. Phys. **107**, 6756 (1997).  
[6] R. Q. Chen and H. Guo, J. Chem. Phys. **105**, 1311 (1996).  
[7] H. G. Yu and S. C. Smith, Ber. Bunsenges. Phys. Chem. **101**, 400 (1997).  
[8] J. W. Pang, D. Neuhauser, and N. Moiseyev, J. Chem. Phys. **106**, 6839 (1997).  
[9] E. Narevicius, H. J. Korsch, D. Neuhauser and N. Moiseyev, Chem. Phys. Lett. **276**, 250 (1997).  
[10] U. Peskin and N. Moiseyev, J. Chem. Phys. **99**, 4590 (1993).  
[11] For a review, see N. Moiseyev, Comments At. Mol. Phys. **31**, 87 (1995), and references therein.  
[12] G. B. Berman, G. M. Zaslavsky, and A. R. Kolovsky, Zh. Éksp. Teor. Fiz. **81**, 506 (1981) [Sov. Phys. JETP **54**, 272 (1981)].  
[13] A. R. Kolovsky, Phys. Lett. A **157**, 474 (1991).  
[14] A. R. Kolovsky, in *Chaos—The Interplay Between Stochastic and Deterministic Behaviour*, edited by P. Garbaczewski, M. Wolf, and A. Weron (Springer, Berlin, 1995).  
[15] N. Moiseyev, H. J. Korsch, and B. Mirbach, Z. Phys. D **29**, 125 (1994).  
[16] V. Averbukh, N. Moiseyev, B. Mirbach, and H. J. Korsch, Z. Phys. D **35**, 247 (1995).  
[17] T. Gorin, H. J. Korsch, and B. Mirbach, Chem. Phys. **217**, 147 (1997).